



Phthalate debranched *Canna edulis* Ker starch with high degree of substitution: preparation, characterization and property

Tang Hongbo¹ · Zhao Qian¹ · Li Yanping¹ · Liu Xiaojun¹

Received: 23 February 2021 / Revised: 26 May 2021 / Accepted: 18 October 2021 /
Published online: 8 November 2021

© The Author(s), under exclusive licence to Springer-Verlag GmbH Germany, part of Springer Nature 2021

Abstract

Debranched *Canna edulis* Ker starch (DCEKS) was effectively esterified in 1-butyl-3-methylimidazolium chloride (ionic liquid) to shorten the esterification time of phthalic anhydride and enhance the substitution degree. The results indicated that the esterification of phthalic anhydride obviously improved the thermal stability of CEKS, while the debranching slightly increased the thermal stability of CEKS. DCEKS was still a semicrystalline polymer like CEKS, and its crystalline structure was not changed by the debranching, but phthalate debranched *Canna edulis* Ker starch (PDCEKS) was almost an amorphous polymer due to the high esterification in the ionic liquid. The esterification decreased the average size of DCEKS, whereas the debranching increased the average size. The esterification was unevenly completed on DCEKS particles. Both debranching and esterification could result in a decrease in the freeze–thaw stability, swelling power and viscosity of CEKS. The stretching vibration of benzene rings appeared at the wave numbers of 1598 cm^{-1} , 1077 cm^{-1} and 640 cm^{-1} .

Keywords *Canna edulis* ker starch · Esterification · Debranching · Structure · Property

Introduction

Starch is one of the most abundant polysaccharides in nature [1], and widely used as a thickener, colloidal stabilizer, gelling agent, bulking agent, and water retention agent in food, medical and industrial fields [2, 3]. Starch consists of amylose, which is essentially a linear molecule containing glucose unit linked by α -1, 4 linkages

✉ Tang Hongbo
tanghb6666@sina.com

¹ School of Environmental and Chemical Engineering, Shenyang University of Technology, Shenyang 110870, China

with a few branches, and amylopectin, which is highly α -1, 6 branched and has the large molecular weight [4]. *Canna edulis* Ker starch (CEKS) is extracted from *C. edulis*, which is cultivated in many regions [5]. Consequently, CEKS like other starches is able to be modified physically, chemically, biologically and radioactively in order to get a wider application [6, 7]. Although a single modified starch satisfies the functional properties required in some applications, it still does not overcome some undesirable properties. Therefore, the compound modification is adopted further to improve the undesirable characteristics of starch.

The debranching is one of enzyme modifications, by which the ratio of amylose to amylopectin is able to be fundamentally changed. The debranching is completed at α -1, 6 linkages by the debranching enzymes such as isoamylase and pullulanase, which specifically cleaves α -1,6-glucosidic bonds in glucans containing both α -1,4 and α -1,6 linkages [8]. As a result, the debranched starch will have some functional properties that the ordinary starch does not have as increasing the debranching degree. Accordingly, it is often used as a fat replacer, coating material and medicine excipient [9]. As reported, the debranching improves the film-forming property, anti-digestibility, gel performance of starch, but decreases its viscosity, freeze–thaw stability, water holding capacity, swelling capacity, etc.

The esterification belongs to one of chemical modifications which generally include the oxidation [10], cross-linking [11], esterification [12], etherification [13], acidolysis [14] and graft [15]. The common esterifying agents are usually sodium tripolyphosphate [16], acetic anhydride [17], maleic anhydride [18], vinyl acetate [19], octenyl succinic anhydride [20], chlorosulfonic acid [21] and so on. The esterified starch shows the different functional performances due to the introduction of the different groups and the increase in the substitution degree. Normally, the high esterification of certain compounds such as acetic anhydride, octenyl succinic anhydride and phthalic anhydride can improve the plasticity and hydrophobicity of starch [12, 22]. However, compared with other esterified starch, phthalate starch can have a better adhesion to aromatic polyesters and will become a promising enteric coating material.

Recently, many researches indicated that the high modification of starch had to be achieved in organic solvents, and the process took a long time to do so. The ionic liquids (ILs) as the most promising solvents can well replace the volatile organic reagents commonly used in various processes and syntheses owing to its odorless, non-flammability, very low vapor pressure, good thermal and chemical stability, and significantly enhance the reaction efficiency [23].

In this work, a combination modification of pullulanase debranching and phthalic anhydride esterification in 1-butyl-3-methylimidazolium chloride was chosen to functionalize CEKS in order to improve well CEKS performances. Meantime, the influence of debranching and esterification on the structure and properties of CEKS was investigated so that phthalate debranched *Canna edulis* Ker starch (PDCEKS) could be well utilized in some special fields.

Materials and methods

Materials

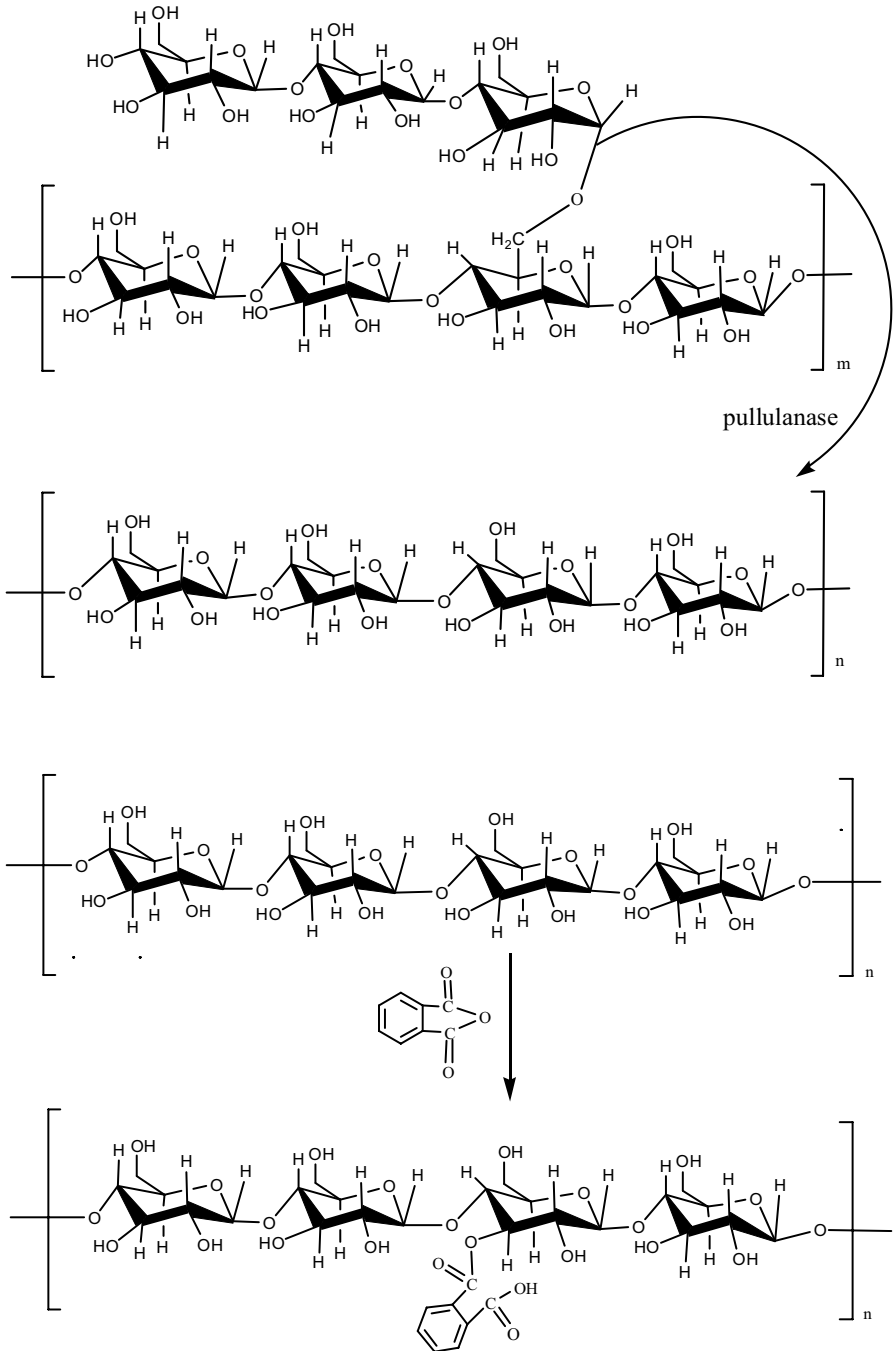
Canna edulis Ker starch (Amylose content = 28.9%) was supplied by the Zhenkang Shengyuan Economy and Trade Co, Ltd (China), and it was purified using the previously published procedure [24]. 1-butyl-3-methylimidazolium chloride (ionic liquid) was supplied by CAS Lanzhou Institute of Chemical Physics. Pullulanase was supplied by Cangzhou Xia Sheng Enzyme Biotechnology Co. Ltd. Phthalic anhydride was supplied by Tianjin Damao Chemical Reagent Factory (China). Other reagents such as sodium hydroxide, hydrochloric acid, iodine, potassium iodide, ethanol and potassium bitartrate were analytical.

Preparation of phthalate debranched *canna edulis* ker starch (PDCEKS)

The emulsions with a mass concentration of 10% (w/w) was produced blending 35 g *Canna edulis* Ker starch (CEKS, Water content = 13.7%, the water content was measured by an Ohaus MB25 Quick moisture analyzer) with 0.2 mol/L citric acid-sodium citrate buffer (pH = 4.5) in a 500-mL three-necked flask equipped with a stirrer, heated to 90 °C in a water bath and kept the constant temperature for 40 min until starch was completely gelatinized. After the paste was cooled to 55 °C, 800 U/g pullulanase (Based on dry *Canna edulis* Ker starch) was added into the paste. After 3 h of debranching, the paste was heated to 100 °C for 30 min to inactivate the enzyme. A certain excess anhydrous ethanol was added to precipitate the debranched starch. Afterward, the debranched *Canna edulis* Ker starch (DCEKS) was acquired by a centrifugation, washing, drying, crushing, sieving [25].

36 g 1-butyl-3-methylimidazolium chloride (ionic liquid) was accurately weighed and placed in a 100-mL three-necked flask equipped with a stirrer, heated to 120 °C in an oil bath, and then 3 g DCEKS (DE = 0.21) was added into the ionic liquid. After mechanically stirring for 30 min, a certain amount of phthalic anhydride (the percent ratio of phthalic anhydride to dry DCEKS was 250%) was added into the mixture. After 4 h of the reaction, the excess distilled water was added into the mixture to precipitate the product. The phthalate debranched *Canna edulis* Ker starch (PDCEKS) was got by a centrifugation, washing (3–4 times), drying, crushing, sieving [26].

The schematic diagram of debranching and phthalic anhydride esterification was as follows:



Determination of debranching degree and substitution degree

The debranching degree of CEKS was evaluated with the dextrose equivalent (DE), which was determined by a DNS (3, 5-dinitrosalicylic acid) colorimetry method [27]. The functional relationship between absorbance (Y) and glucose content (x) was as follows:

$$Y = 0.00314 + 1.287x \quad (1)$$

The DE of samples was calculated as the following formula:

$$DE = \frac{\text{Reducing sugar in starch hydrolysate (expressed as glucose)}}{\text{Total solids content of starch hydrolysate}} \times 100 \quad (2)$$

The degree of substitution (DS) of PDCEKS was determined according to a previously mentioned method [28]. 1.00 g dry PDCEKS and 10 mL 75% (v/v) ethanol solution were added into a conical bottle. After evenly dispersing, 10 mL 0.1 mol/L NaOH solution was added, and the saponification was carried out at 30 °C for 4 h. Then, a few drops of phenolphthalein as indicator was added into the suspension, next, 0.1 mol/L HCl solution was titrated into the suspension until the red color disappeared. The blank titration of the same amount of DCEKS was carried out as the above operation. The DS was calculated by the following formula:

$$W_P = \frac{149 C (v_0 - v_1)}{1000 \times W} \times 100\% \quad (3)$$

$$DS = \frac{162W_P}{149 \times (100 - W_P)} \quad (4)$$

where, W_P is the content of phthalate substituted (%), C is the concentration of hydrochloric acid solution ($\text{mol}\cdot\text{L}^{-1}$), V_0 and V_1 are the volumes of hydrochloric acid solution consumed by DCEKS and PDCEKS during titration (mL), W is the weight of sample (g).

Freeze–thaw stability, blue value and swelling power

80 g 4% (w/w) milk was accurately produced mixing 32 g dry sample and 48 g distilled water in a beaker, heated to 95 °C in water bath and kept the constant temperature for 20 min (Keeping the total weight unchanged during the gelatinization), and then slowly cooled to 25 °C. Afterward, the paste was poured into five pre-weighed 10 mL centrifugal tubes, and weighed. These centrifugal tubes were placed in a refrigerator and frozen at -20 °C for 24 h, and thawed in water at 30 °C for 2 h, and centrifuged at 3000 r/min 20 min. The freeze–thaw stability (Measured by syneresis rate) was calculated according to following formula [29]:

$$\text{Syneresis rate} = \frac{m_1}{m} \times 100\% \quad (5)$$

where, m_1 is the mass of separated water after thawing (g), m is the mass of the paste before freezing (g).

50 mL 0.5 mg/mL emulsion was prepared in a conical flask and heated in water bath until the sample was completely gelatinized, and cooled to the room temperature. 1 mL paste was pipetted and placed in a 50-mL volumetric flask, 0.07–0.1 g potassium tartrate and 0.5 mL iodine solution (2 mg/mL iodine, 20 mg/mL potassium iodide) were added into the paste, and then suitable water added to the total volume of 50 mL. Finally, the absorbance of the mixture was measured at 600 nm, and the blue value was calculated according to following formula [30]:

$$\text{Blue value} = \frac{4 \times \text{Absorbance}}{10 \times C} \quad (6)$$

where, C is the concentration of sample (mg/L).

50 g 4% (w/w) emulsion was produced to determine the swelling power of samples, heated to 85 °C and kept the constant temperature for 30 min, and then put four graduated centrifuge tubes and centrifuged at 3000 r/min for 30 min. The precipitate was separated from the supernatant. And then the precipitate and supernatant were collected separately in a Petri dish, dried to the constant weight and accurately weighed. The swelling power of samples was calculated according to following formula [31]:

$$S = \frac{A}{W} \times 100 \quad (7)$$

$$\text{Swelling power}(\%) = \frac{P \times 100}{m(100 - S)} \quad (8)$$

where, S is the solubility (%); A is the mass of dried residue of supernatant (g); P is the mass of sediment paste (g); m is the mass of dry sample (g).

Characterization

An IR Prestige-21 infrared spectrometer (Shimadzu Corporation, Japan) was used to record FTIR spectra of samples within the range of 4000–400 cm^{-1} [32]. A Q50 V20.10 Build 36 thermogravimetric analyzer (TA Instruments, US) was used to perform the thermal properties of samples [33]. A MCR102 rheometer (Anton Paar, Austria) was used to determine the pasting characteristics of samples with a mass concentration of 4% (w/w). The initial speed of blender in first 10 s was 960 rpm, the speed of blender was maintained at 160 rpm [34]. A MiniFlex600 X-ray diffractometer (Rigaku Corp, JP) was used to analyze the crystalline structure at voltage 40 kV, current 15 mA, scanning rate 2°/min and scanning angle range 5–50° [35]. The XRD curves were analyzed by MDI Jade 6.5 software. The crystalline degree of samples was calculated as following equation.

$$X_c = \frac{A_c}{A_c + A_a} \times 100 \quad (9)$$

where, X_c is the crystalline degree (%), A_c is the area of crystallization zone (mm^2), A_a is the area of amorphous zone (mm^2).

A Hitachi S-3400 N scanning electron microscope was used to observe the morphology of samples [36]. A Mastersizer 3000 (Malvern Panalytical Ltd., UK) was used to measure the size distribution of samples by a dry method [37].

Results and discussion

Effect of esterification time, amount of phthalic anhydride, esterification temperature and amount of ionic liquid on DS

The effect of esterification time, amount of phthalic anhydride, esterification temperature and amount of ionic liquid on DS was shown in Fig. 1. The amount of phthalic anhydride and ionic liquid was defined as the percentage mass ratio of phthalic anhydride and ionic liquid to dry DCEKS. From Fig. 1a, the amount of phthalic anhydride had a great influence on the DS of PDCEKS. The DS of PDCEKS increased as increasing the amount of phthalic anhydride. When the amount of phthalic anhydride was more than 350%, the increase in DS of PDCEKS became slow. It should relate to the steric hindrance effects of benzene ring gradually appearing as increasing DS of PDCEKS. Considering the use of PDCEKS, the amount of phthalic anhydride was chosen as 250%.

From Fig. 1b, when the esterification time was less than 4 h, the DS of PDCEKS increased as increasing the esterification time. When the esterification time was greater than 4 h, the DS of PDCEKS did not increase. It was suggested that the esterification time of 4 h could meet the esterification of DCEKS in the ionic liquid. Therefore, the suitable esterification time was 4 h. Although the esterification time was longer than that provided by literature, the solvent used in the modification of PDCEKS was completely different from the solvent used in this literature [38].

From Fig. 1c, the effect of esterification temperature on the DS of PDCEKS was similar to that of esterification time. The esterification temperature 120 °C is the inflection point on the relationship curve between esterification temperature and DS of PDCEKS. Interestingly, when the esterification temperature was greater than 120 °C, the DS of PDCEKS did not change. Therefore, the suitable esterification temperature was 120 °C.

From Fig. 1d, the effect of the amount of ionic liquid on the DS of PDCEKS was less than that of esterification time and amount of phthalic anhydride, and the DS of PDCEKS only varied from 0.568 to 0.761 within the change range of ionic liquid. When the amount of ionic liquid was less than 1200%, the DS of PDCEKS increased as increasing the amount of ionic liquid. When the amount of ionic liquid was greater than 1200%, the DS of PDCEKS decreased as increasing the amount of ionic liquid. Therefore, the suitable amount of ionic liquid was 1200%.

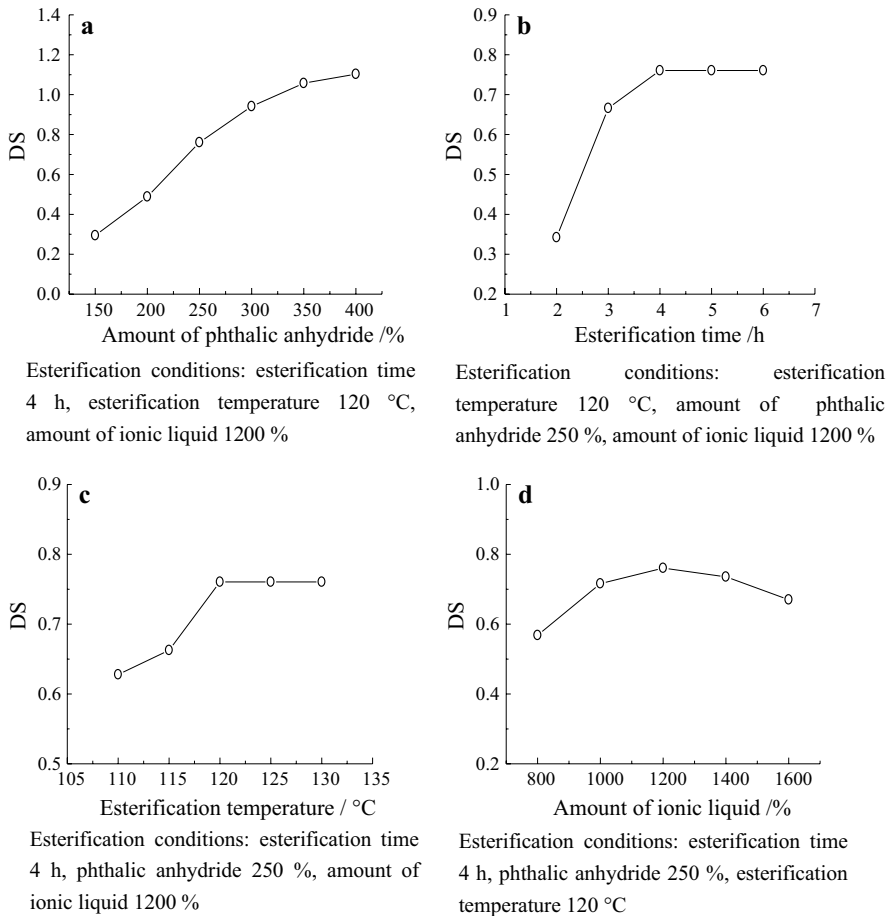


Fig. 1 Effect of amount of phthalic anhydride (a), esterification time (b), esterification temperature (c) and amount of ionic liquid (d) on DS

Effect of debranching and esterification on freeze–thaw stability, blue value and swelling power of CEKS

The freeze–thaw stability, blue value and swelling power of CEKS, DCEKS (DE=0.21) and PDCEKS (DE=0.21, DS=0.760) were shown in Table 1. From Table 1, after the debranching and esterification of CEKS, the syneresis rate of its derivatives increased, confirming that the debranching and esterification reduced the freeze–thaw stability. The reduction in the freeze–thaw stability caused by debranching and esterification should relate to the increase in the short linear chains and introduction of hydrophobic groups into the molecular chains of starch because the increase in short linear chains and introduction of hydrophobic groups weakened the water holding capacity. In fact, the result of poor water holding capacity caused by short linear chains was also given in the literature [39]. The debranching increased

Table 1 Effect of debranching and esterification on freeze–thaw stability, blue value and swelling power

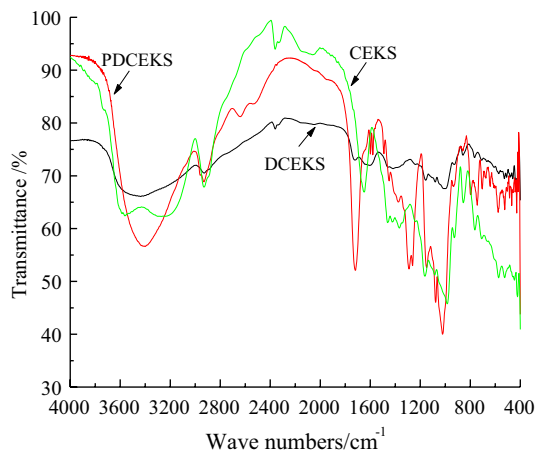
Samples	Synersis rate /%	Blue value	Swelling power (65 °C) /%	Swelling power (75 °C) /%	Swelling power (85 °C) /%
CEKS	53.0	0.268	9.3	13.9	15.8
DCEKS	79.7	0.316	6.3	7.9	8.6
PDCEKS	96.7	0.036	2.1	2.5	2.7

the blue value of CEKS, while the esterification significantly reduced the blue value. The swelling power of CEKS, DCEKS and PDCEKS increased as increasing the temperature, and the debranching and esterification decreased the swelling power of CEKS. The latter should be related to the increase in the short chains caused by debranching and the introduction of hydrophobic groups due to the esterification. Compared with long starch chains, the short linear chains were beneficial to the aggregation to form a gel leading to a reduction in starch swelling power. The result of the change in swelling power caused by debranching was consistent with the result observed in the literature [40].

Analysis of infrared spectroscopy

The FTIR spectra of CEKS, DCEKS (DE=0.21) and PDCEKS (DE=0.21, DS=0.760) were shown in Fig. 2. From Fig. 2, the stretching vibration of O–H and C–H bonds showed the absorption peaks at 3407 cm⁻¹, 2923 cm⁻¹, respectively. The stretching vibration peaks of the C–O–C bonds and bending vibration peaks of the C–O–H bonds showed at 1163 cm⁻¹, 1070 cm⁻¹, separately. PDCEKS FTIR included two characteristic peaks, namely the stretching vibration of carbonyl bonds and phenyl groups. The stretching vibration of C=O groups appeared at 1720 cm⁻¹, and its intensity was the strongest among all peaks. The similar observation was

Fig. 2 FTIR spectra of CEKS, DCEKS and PDCEKS



reported in the literature [41]. The stretching vibration of benzene rings showed at 1598 cm^{-1} , 1077 cm^{-1} and 640 cm^{-1} . The result was in accordance with the result reported in the literature [42]. The absorption peak at 1288 cm^{-1} and 1024 cm^{-1} should be in-plane bending vibration of C–H bonds in benzene ring. It proved that the phthalate groups were successfully introduced into DCEKS molecular chains. The intensity of all absorption peaks of DCEKS became weaker than that of CEKS, especially the intensity of absorption peak at 991 cm^{-1} was very weaker. It confirmed that the crystalline structure of DCEKS was completely different from that of CEKS, namely the debranching changed the crystalline structure of CEKS.

SEM analysis

The SEM photographs of CEKS, DCEKS (DE=0.21) and PDCEKS (DE=0.21, DS=0.760) were shown in Fig. 3. From Fig. 3, the surface of CEKS was smooth

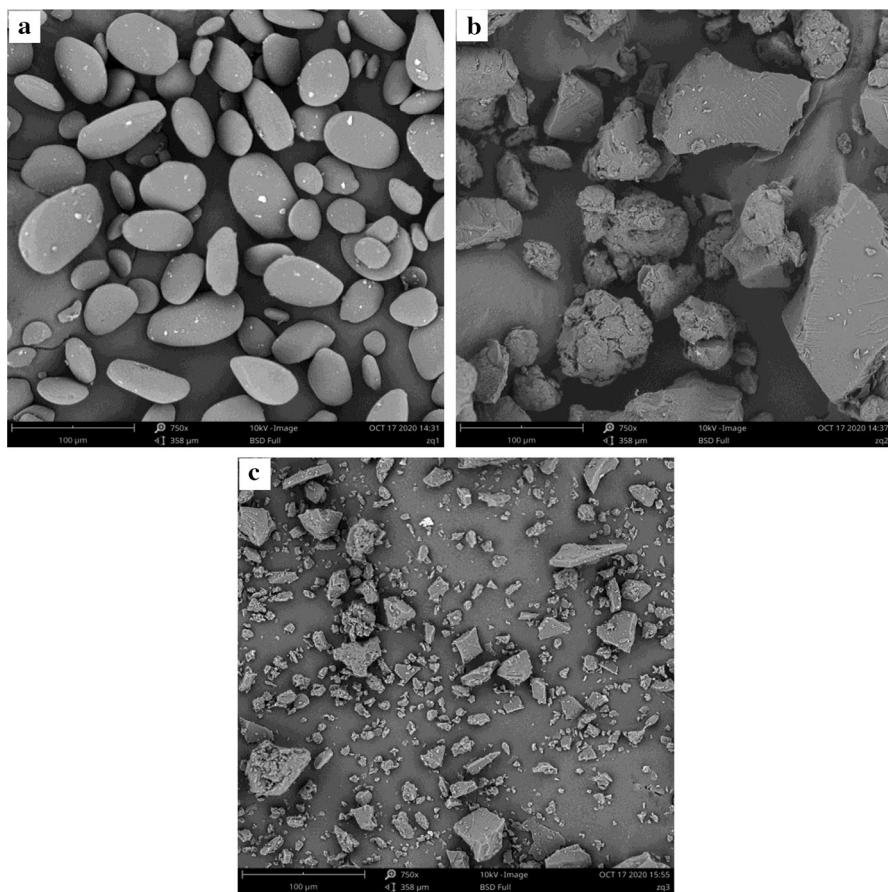


Fig. 3 SEM photos of CEKS (a), DCEKS (b) and PDCEKS (c)

except for some very small particles, and most of CEKS particles were elliptical. After the debranching of CEKS, the surface of some DCEKS particles became very rough, while the surface of other particles was still smooth. DCEKS particles were irregular, and some particles were larger in size than the native CEKS. After the esterification of DCEKS, many small particles appeared, but some large particles could be still seen. The surface of some particles became rougher than DCEKS, while the surface of other particles remained smooth. It was suggested that the esterification was uneven.

Analysis of TGA and XRD

The TGA and XRD curves of CEKS, DCEKS (DE=0.21) and PDCEKS (DE=0.21, DS=0.760) were shown in Fig. 4. From Fig. 4 a, the debranching and esterification changed the thermal properties. The water loss section of DCEKS and PDCEKS was clearly different from that of CEKS. Interestingly, the water loss section of PDCEKS was an oblique line, confirming that water in PDCEKS was not easily evaporated as increasing the temperature. The debranching and esterification move TGA curves of DCEKS and PDCEKS to the left. As a result, the initial decomposition temperature of DCEKS and PDCEKS was reduced. Meanwhile, the debranching and esterification also slowed down the slope of rapid decomposition stage, confirming that the thermal stability of DCEKS and PDCEKS was greater than that of CEKS. Furthermore, the TGA thermodynamics key parameters of CEKS, DCEKS and PDCEKS were calculated and listed in Table 2 to analyze further these curves.

From Table 2, the debranching lowered the onset decomposition temperature and end decomposition temperature of CEKS. However, the esterification enhanced the onset decomposition temperature and end decomposition temperature of DCEKS. In addition, the sequence of mass loss rate was: CEKS > DCEKS > PDCEKS, that is, the sequence of the thermal stability was PDCEKS > DCEKS > CEKS. It was suggested that the effect of the debranching on the thermal stability was inconsistent with that of the esterification.

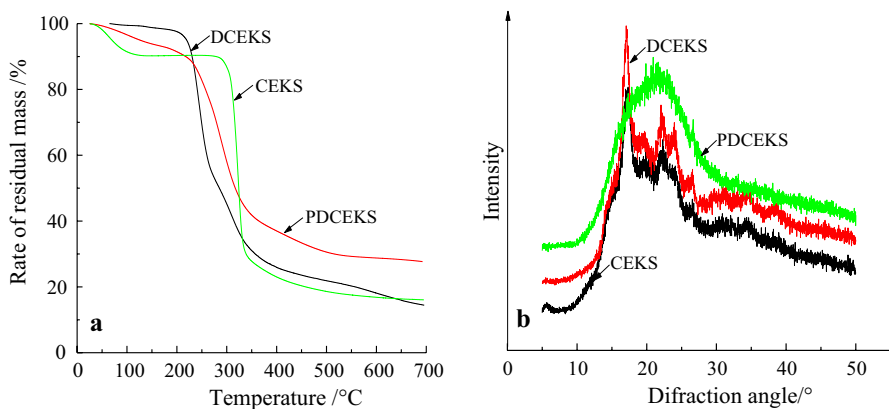


Fig. 4 TGA (a) and XRD (b) curves of CEKS, DCEKS and PDCEKS

Table 2 TGA thermodynamics key parameters of CEKS, DCEKS and PDCEKS

Samples	CEKS	DCEKS	PDCEKS
Onset decomposition temperature /°C	307.0	222.1	244.0
End decomposition temperature /°C	335.2	293.1	346.4
Mass loss rate /%	50.0	47.8	42.4

From Fig. 4b, the diffraction peaks of CEKS appeared at diffraction angles of 17.1°, 19.7°, 22.2°, 23.9°, 26.3°, 31.2°, 34.4°, respectively, and confirming that the crystalline structure of CEKS was typically a B-type. The result was consistent with the result provided in the literature [43]. The diffraction peaks of DCEKS were same as those of CEKS except for the different intensities of some peaks, confirming that the crystalline structure of DCEKS was changed by debranching. However, after the esterification, the crystalline structure of PDCEKS was transformed into an amorphous structure. The result was consistent with the result described by the literature [44]. Furthermore, the crystalline degree of CEKS, DCEKS and PDCEKS was calculated to be 15.6%, 19.2%, 0, separately.

Effect of debranching and esterification on gelatinization properties

The gelatinization curves of CEKS, DCEKS (DE=0.21) and PDCEKS (DE=0.21, DS=0.760) were shown in Fig. 5. From Fig. 5, the gelatinization curve of CEKS was distinctly affected by the debranching and esterification. The viscosity of DCEKS was significantly lower than that of CEKS. The result was consistent with the result reported in literature [45]. The viscosity of CEKS hardly decreased during the gelatinization, which was different from that of corn starch and potato starch. After the conclusion of the constant temperature of 95 °C, the viscosity of CEKS increased rapidly as lowering the temperature. The viscosity of DCEKS hardly changed during the gelatinization, while the viscosity of PDCEKS changed. The viscosity of PDCEKS increased like CEKS after the constant temperature of 95 °C was over. The key gelatinization parameters of CEKS, DCEKS and PDCEKS were given in Table 3 to deeply discuss the effect of debranching and esterification on the gelatinization properties.

From Table 3, the breakdown of CEKS was only 30.3 cP, but its setback reached a value of 785.3 cP. It was confirmed that the paste of CEKS had a very high shear resistance and strong retrogradation. The peak viscosity, final viscosity, breakdown and setback of PDCEKS were all larger than DCEKS except for the trough viscosity. It was suggested that the esterification enhanced the breakdown and setback of DCEKS. In addition, the low viscosity of DCEKS should relate to its high amylose content composed of original amylose and amylose from debranching.

Effect of debranching and esterification on size distribution

The size distributions of CEKS, DCEKS (DE=0.21) and PDCEKS (DE=0.21, DS=0.760) were shown in Fig. 6 and Table 4. From Fig. 6, the debranching and

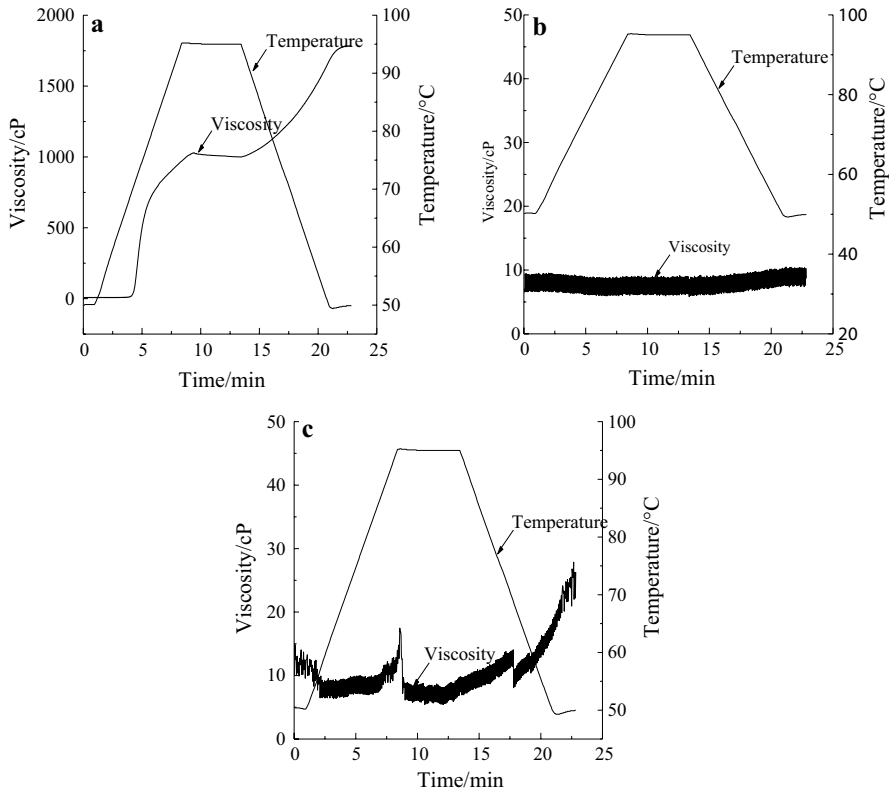


Fig. 5 Gelatinization properties of CEKS (a), DCEKS (b) and PDCEKS (c)

Table 3 Key parameters of CEKS, DCEKS and PDCEKS gelatinization curves

Samples	Pasting temperature /°C	Peak viscosity /cP	Trough viscosity /cP	Final viscosity /cP	Breakdown /cP	Setback /cP
CEKS	69.4	1030.0	999.7	1785.0	30.3	785.3
DCEKS	–	9.5	5.8	8.7	3.7	2.9
PDCEKS	–	17.5	5.4	26.8	12.1	21.4

esterification evidently widened the particle size distributions of DCEKS and PDCEKS. The esterification moved the particle size distributions of PDCEKS to the left and lowered the peak intensity. From Table 4, the sequence of DV (10) and DV (50) was in order of DCEKS, CEKS and PDCEKS, while the sequence of DV (90) was in order of DCEKS, PDCEKS and CEKS. And the DV (10) of PDCEKS was only 6.69 μm, which was much less than the DV (10) of DCEKS and CEKS, and the DV (90) of PDCEKS reached unexpectedly 166.0 μm, which was far greater than DV (90) of DCEKS, but was much smaller than DV (90) of DCEKS. It proved that

Fig. 6 Size distribution of CEKS, DCEKS and PDCEKS

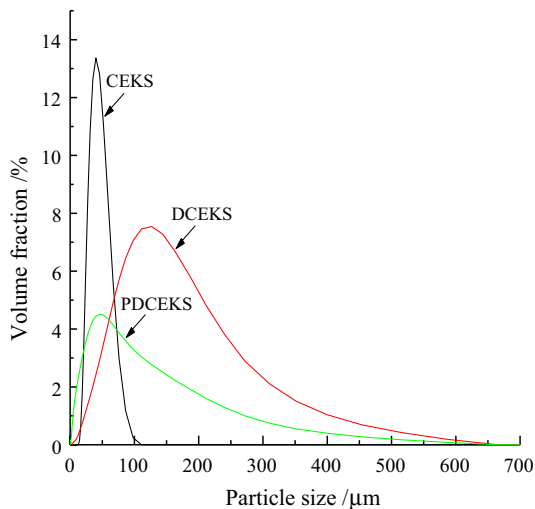


Table 4 Key parameters of size distribution of CEKS, DCEKS and PDCEKS

Samples	Specific surface area / $\text{m}^2 \cdot \text{kg}^{-1}$	Dv(10) / μm	Dv(50) / μm	Dv(90) / μm
CEKS	185.9	26.0	42.4	66.9
DCEKS	80.5	38.8	116.0	262.0
PDCEKS	576.1	6.69	41.7	166.0

the introduction of phenyl groups into the DCEKS molecular chains hindered the regroup of the molecular chains. Moreover, according to the specific surface area, the order of the average size was DCEKS > CEKS > PDCEKS.

Conclusions

The debranching was able to lead to the increase in the blue value, but a reduction in the freeze–thaw stability and swelling power. The esterification could reduce the blue value, freeze–thaw stability and swelling power. The debranching reduced the thermal stability of CEKS, whereas the esterification improved the thermal stability. The esterification of phthalic anhydride was unevenly completed on the DCEKS granules. The debranching and esterification improved the thermal stability of CEKS. The debranching apparently lowered the onset decomposition temperature and end decomposition temperature of CEKS, while the esterification significantly increased these two temperatures. The debranching significantly decreased the viscosity of CEKS. The esterification enhanced the breakdown and setback of DCEKS. The peaks of C=O groups appeared at 1720 cm^{-1} and benzene rings appeared at 1598 cm^{-1} , 1077 cm^{-1} , 640 cm^{-1} indicated that the phthalate groups were successfully inserted into DCEKS molecular chains. The crystalline structure of CEKS

and DCEKS was typically a B-type, and the crystalline structure of PDCEKS was an amorphous structure. The phenyl groups hindered the regroup of the molecular chains according to the size of PDCEKS particles.

Acknowledgements Authors are grateful to individuals who have supported their research.

Declarations

Conflict of interest All authors declare that they have no known competing conflict of interest or personal relationships that can appear to influence the work reported in this paper.

References

1. Haroon M, Wang L, Yu H, Abbasi NM, Zain-ul-Abdin ZA, Saleem M, Wu J (2016) Chemical modification of starch and its application as an adsorbent material. *RSC Adv* 6(82):78264–78285
2. Singh J, Kaur L, McCarthy OJ (2007) Factors influencing the physico-chemical, morphological, thermal and rheological properties of some chemically modified starches for food applications-A review. *Food Hydrocolloids* 21:1–22
3. Bamidele OP, Duodu KG, Emmambux MN (2018) Encapsulation and antioxidant activity of ascorbyl palmitate with normal and high amylose maize starch by spray drying. *Food Hydrocolloids* 86:124–133
4. Kittiwut T, Dudsadee U, Kuakoon P, Yasuhito T (2003) A comparative study of edible canna (*Canna edulis*) starch from different cultivars. Part II. Molecular structure of amylose and amylopectin. *Carbohydr Polym* 54(4):489–498
5. Zhang J, Wang ZW, Yang JA (2010) Physicochemical properties of canna edulis ker starch on heat-moisture treatment. *Int J Food Prop* 13(6):1266–1279
6. Ociecek A, Skotnicka M, Baranowska K (2017) Sorptive properties of modified maize starch as indicators of their quality. *Int Agrophys* 31(3):383–392
7. Ai Y, Jane J (2015) Gelatinization and rheological properties of starch. *Starch/Stärke* 67(3–4):213–224
8. Klaochanpong N, Puttanlek C, Rungsardthong V, Puncha-arnon S, Uttapap D (2015) Physicochemical and structural properties of debranched waxy rice, waxy corn and waxy potato starches. *Food Hydrocolloids* 45:218–226
9. Liu G, Gu Z, Hong Y, Cheng L, Li C (2017) Structure, functionality and applications of debranched starch: A review. *Trends Food Sci Technol* 63:70–79
10. Haaksman IK, Besemer AC, Jetten JM, Timmermans JW, Slaghek TM (2006) The oxidation of the aldehyde groups in dialdehyde starch. *Starch/Stärke* 58(12):616–622
11. Shi M, Gu F, Wu J, Yu S, Gao Q (2013) Preparation, physicochemical properties, and in vitro digestibility of cross-linked resistant starch from pea starch. *Starch/Stärke* 65(11–12):947–953
12. Li P, He X, Zuo Y, Li X, Wu Y (2020) Synthesis and characterization of lactic acid esterified starch by an in-situ solid phase method. *Int J Biol Macromol* 156:1316–1322
13. Misman MA, Azura AR, Hamid ZAA (2015) Physico-chemical properties of solvent based etherification of sago starch. *Ind Crops Prod* 65:397–405
14. Wang XM, Zhang YM (2013) Study on one-step process of the size mixture blending and acidolysis modification of starch. *Adv Mater Res* 2735:1122–1125
15. Worzakowska M (2018) Chemical modification of potato starch by graft copolymerization with citronellyl methacrylate. *J Polym Environ* 26(4):1613–1624
16. Zhang X, Luo L, Kang H, Liu X, Zhu W, Yu X (2016) Preparation of edible corn starch phosphate with highly reactive sodium tripolyphosphate in the absence of catalyst. *Trop J Pharm Res* 15(3):441–445
17. Singh N, Chawla D, Singh J (2003) Influence of acetic anhydride on physicochemical, morphological and thermal properties of corn and potato starch. *Food Chem* 86(4):601–608
18. Zuo Y, Gu J, Yang L, Qiao Z, Tan H, Zhang Y (2013) Synthesis and characterization of maleic anhydride esterified corn starch by the dry method. *Int J Biol Macromol* 62:241–247

19. Ramaraj B, Shit SC, Nayak SK (2012) Effect of ethylene vinyl acetate on physico-mechanical and thermal properties of polypropylene and starch biocomposites. *J Elastomers Plast* 44(6):515–531
20. No J, Shin M (2019) Preparation and characteristics of octenyl succinic anhydride-modified partial waxy rice starches and encapsulated paprika pigment powder. *Food Chem* 295:466–474
21. Abd El-Rehim HA, Hegazy ESA, Diao DA (2013) Radiation synthesis of eco-friendly water reducing sulfonated starch/acrylic acid hydrogel designed for cement industry. *Radiat Phys Chem* 85:139–146
22. Amin MR, Anannya FR, Mahmud MA, Raian S (2019) Esterification of starch in search of a biodegradable thermoplastic material. *J Polym Res* 27(21):98–107
23. Wu Y, Sasaki T, Irie S, Sakurai K (2008) A novel biomass-ionic liquid platform for the utilization of native chitin. *Polymer* 49(9):2321–2327
24. Pauly A, Pareyt B, De Brier N, Fierens E, Delcour JA (2012) Starch isolation method impacts soft wheat (*Triticum aestivum* L. cv. Claire) starch puroindoline and lipid levels as well as its functional properties. *J Cereal Sci* 56(2):464–469
25. Zhang B, Qiang H, Luo FX, Xiong F (2012) Structural characterizations and digestibility of debranched high-amylose maize starch complexed with lauric acid. *Food Hydrocolloids* 28(1):174–181
26. Ashamol A, Priyambika VS, Avadhani GS, Sailaja RRN (2013) Nanocomposites of crosslinked starch phthalate and silane modified nanoclay: Study of mechanical, thermal, morphological, and biodegradable characteristics. *Starch/Stärke* 65(5–6):443–452
27. Tang H, Liu L, Li Y, Dong S (2015) Debranching potato starch: synthesis, optimization and thermal property. *Polym Bull* 72(10):2537–2552
28. Sun Y, Hu Q, Qian J, Li T, Ma P, Shi D, Dong W, Chen M (2016) Preparation and properties of thermoplastic poly(caprolactone) composites containing high amount of esterified starch without plasticizer. *Carbohydr Polym* 139:28–34
29. Reddy I, Seib PA (2000) Modified waxy wheat starch compared to modified waxy corn starch. *J Cereal Sci* 31:25–39
30. Xia X, Li G, Liao F, Zhang F, Zheng J, Kan J (2015) Granular structure and physicochemical properties of starches from amaranth grain. *Int J Food Prop* 18:1029–1037
31. Yu SF, Ma Y, Menager L, Sun D (2012) Physicochemical properties of starch and flour from different rice cultivars. *Food Bioprocess Technol* 5:626–637
32. Černá M, Barros AS, Nunes A, Rocha SM, Delgado I, Čopíková J, Coimbra MA (2003) Use of FT-IR spectroscopy as a tool for the analysis of polysaccharide food additives. *Carbohydr Polym* 51:383–389
33. Tian Y, Li Y, Xu X, Jin Z (2011) Starch retrogradation studied by thermogravimetric analysis (TGA). *Carbohydr Polym* 84(3):1165–1168
34. Reddy CK, Pramila S, HariPriya S (2015) Pasting, textural and thermal properties of resistant starch prepared from potato (*Solanum tuberosum*) starch using pullulanase enzyme. *J Food Sci Technol* 52(3):1594–1601
35. Pal P, Pandey JP, Sen G (2018) Grafted sesbania gum: A novel derivative for sugarcane juice clarification. *Int J Biol Macromol* 114:349–356
36. Sujka M, Jamroz J (2013) Ultrasound-treated starch: SEM and TEM imaging and functional behavior. *Food Hydrocolloids* 31(2):413–419
37. Qi W, Liang X, Yun T, Guo W (2019) Growth and survival of microencapsulated probiotics prepared by emulsion and internal gelation. *J Food Sci Technol* 56(3):1398–1404
38. Ashamol A, Sailaja RRN (2012) Mechanical, thermal, and biodegradation studies of polystyrene-phthalated starch blends using epoxy functionalized compatibilizer. *J Appl Polym Sci* 125:313–326
39. Liu G, Yan H, Gu Z, Li Z, Li C (2015) Pullulanase hydrolysis behaviors and hydrogel properties of debranched starches from different sources. *Food Hydrocolloids* 45:351–360
40. Cao C, Shen M, Hu J, Qi J, Xie P, Zhou Y (2020) Comparative study on the structure properties relationships of native and debranched rice starch. *CyTA - J Food* 18(1):84–93
41. Chooprayoon P, Boochathum P (2019) Self-crosslinkable hydroxylated natural rubber/carboxymethyl starch blend and its properties. *Appl Polym* 136:47271–47280
42. Nobrega MM, Olivato BJ, Muller MOC, Yamashita F (2012) Biodegradable starch-based films containing saturated fatty acids: thermal, infrared and raman spectroscopic characterization. *Polímeros* 22:475–480
43. Zhang J, Wang ZW, Shi XM (2009) Effect of microwave heat/moisture treatment on physicochemical properties of *Canna edulis* Ker starch. *J Sci Food Agric* 89(4):653–664

44. Liu G, Hong Y, Gu Z (2013) Evaluation of amorphous debranched starch as extended-release matrices in tablets. *Carbohydr Polym* 98(1):995–1001
45. Tang H, Qu Y, Li Y, Dong S (2018) Synthesis of hydroxypropylated debranched pea starch with high substitution degree in an ionic liquid, and its characterization and properties. *J Polym Res* 25(11):235–245

Publisher's Note Springer Nature remains neutral with regard to jurisdictional claims in published maps and institutional affiliations.